JOURNAL OF BIOMEDICAL OPTICS 3(3), 346–356 (JULY 1998)

METAL ION QUENCHING KINETICS OF DTDCI IN VISCOUS SOLUTION AND NAFION MEMBRANES: MODEL SYSTEM FOR NEAR INFRARED FLUORESCENCE SENSING

Olaf J. Rolinski, David J. S. Birch, and A. Sheila Holmes
Strathclyde University, Department of Physics and Applied Physics, 107 Rottenrow, Glasgow G4 ONG, Scotland, United Kingdom

(Paper JBO-89 received Aug. 12, 1996; revised manuscript received Sep. 22, 1997; accepted for publication Jan. 12, 1998.)

ABSTRACT

Förster type energy transfer offers opportunities as a sensitive and frequently selective method of monitoring the concentration of analytes in medical sensing applications. However, the fluorescence quenching kinetics observed in microheterogeneous media such as tissue are likely to be less than ideal. In the present article, the quenching kinetics of the carbocyanine dye DTDCI by transition metal ions in solutions and in the microheterogeneous polymer Nafion (a registered trademark of Dupont Corporation) are reported and compared with a view to understanding the complex fluorescence kinetics likely to be encountered in biological media. © *1998 Society of Photo-Optical Instrumentation Engineers.* [S1083-3668(98)00703-5]

Keywords near infrared dyes; medical sensing; fluorescence quenching; Nafion polymer.

1 INTRODUCTION

Fluorescence lifetime sensors provide the opportunity for a wide range of applications in biology and medicine. The recently reported glucose sensor[1] based on fluorescence resonance energy transfer and phase-modulation measurements of the fluorescent donor decay time serves as a typical example. The potential advantage for medical purposes in sensing with near infrared (NIR) dyes has recently been recognized. Because human skin and tissue absorption and scatter are minimized above 600 nm, fluorescence lifetime measurements with NIR sensing might be used as a convenient monitor of tissue biochemistry.[2–5]

There are several key advantages in using NIR dyes in sensors such as the improvement in sensitivity resulting from low background emission from autofluorescence when using NIR excitation. Moreover, the possibility of utilizing the low cost and small size of diode lasers or light emitting diodes as the excitation source coupled to glass fibers to allow remote analysis of inaccessible regions and analytes makes NIR sensors especially attractive. Other experimental advantages include minimization of the photodecomposition of the region of interest due to the low energy of the photon used, and reduction of the Rayleigh scattering, as it decreases in intensity in proportion to λ^4.

Address all correspondence to David J. S. Birch: djs.birch@strath.ac.uk. The present address of A. Sheila Holmes is Department of Physical Sciences, Glasgow Caledonian University, Cowcaddens Rd., Glasgow G4 OBA, Scotland, UK.

Nevertheless, in spite of these advantages, infrared fluorescence sensing has still been little exploited. There are several instrumental reasons for this. Commonly used lamps in the ultraviolet/visible (UV/VIS) region have poor monochromicity and low intensity in the infrared. Also, they cannot produce very short pulses, although some studies of NIR laser dyes using spark sources have been reported.[6] The other instrumental problem is the choice of a detector which is sensitive in the infrared. In the case of photomultipliers a low work function of the photocathode is required to detect infrared radiation and this means increased thermally induced noise, which is minimized only by constant cooling.

Recent developments in IR instrumentation[7] have enabled many of these problems to be overcome. For example, using diode lasers as a source of excitation offers all the usual advantages associated with lasers, namely high coherence, narrow spectral linewidth, high intensity, and fast pulse generation. Milliwatt powers are now available at low cost down to ~650 nm using diode lasers, which are thus ideal for studying NIR fluorescence. The detectors presently used for NIR studies include conventional photomultipliers, microchannel plate versions, streak cameras, and various types of photodiodes. Despite the many advances which have occurred in semiconductor devices, photomultipliers with extended red response are still most

widely used. Typical examples are the Phillips XP2257B linear focused device and the Hamamatsu R2949 side-window device.

Early studies in the area of NIR sensors concerned the use of NIR dyes for *p*H determination[8] and *in situ* characterization of Nafion polymer films.[3] Typical NIR dyes are: carbocyanines, porphyrins, oxazines, and xanthenes. Carbocyanines are among the most interesting as NIR sensors because their high absorptivity and fluorescence quantum yield enables detection at very low concentrations (down to $\sim 6\times 10^{-20}$ M).[9] The di- and tricarbocyanines have aromatic or heteroaromatic ring structures linked by a polymethine chain possessing conjugated carbon/carbon double bonds. In this article the fluorescence of the carbocyanine dye 3,3′-diethylthiadicarbocyanine iodide (DTDCI) will be discussed.

The difficulties associated with the use of these NIR dyes are the smaller quantum yield when compared to many visible fluorescent dyes[2,3] and the photochemical changes observed in the spectroscopic properties when placed in aqueous solvents or other high polarity solvents. These changes include the appearance of additional bands in the absorption spectra, often attributed to dye molecule aggregation. It has been shown[4,10] that the internal conversion and the *cis/trans* photoisomerization within the polymethine chain are the major nonradiative pathways in polymethine dyes. All these processes are potential obstacles to using carbocyanine dyes in fluorescence sensing. Another drawback is the behavior of the NIR dyes in different matrices. They are frequently photochemically unstable with the fluorescence intensity of the probe decaying to zero within several hours. In particular, the mean lifetimes for freshly prepared and older samples are often different. We have found DTDCI to be one of the most stable carbocyanine dyes and hence we have chosen it for these model studies. Interestingly enough, although there are a number of reports of steady-state fluorescence quenching studies of carbocyanine dyes,[2,4,5] there are few time resolved studies reported, an omission which we hope to correct in the present work.

The application described here is to use DTDCI as the sensor molecule for transition metal ions in different environments. The quenching of DTDCI fluorescence was employed in a Nafion polymer membrane in order to determine ion concentration using Förster type quenching. A metal ion sensor based on Förster energy transfer in the UV/VIS has already been successfully demonstrated[11] and recently extended to the NIR using rhodamine 800 as a fluorophore.[12] In this article we compare the quenching kinetics for metal ions interacting with DTDCI molecules in an isotropic viscous solvent and in a porous polymer (Nafion) as a model sensor medium. Nafion is a model medium for sensing measurements in more ways than one. For example the SO_3^- head groups give a *p*H equivalent to ~12 M sulphuric acid and the microheterogeneous nature produces scattering sites and complex spatial distributions of both fluorophores and the analyte of interest. In short, there are potentially many sources of systematic error needing to be treated before fluorescence lifetime technology can be implemented in a clinical context and in this article we start to address some of these problems in a model system. Although eventually it may be adequate to describe sensing schemes in terms of average fluorescence lifetimes it is likely that, as in many areas of applied science, a deeper understanding is required before useful results are routinely achieved.

2 The Energy Transfer Models

Fluorescence quenching decreases the fluorescence intensity of a given dye. Possible quenching processes include: complex formation (static quenching), collisional (dynamical) quenching, electron transfer, and nonradiative resonance energy transfer.[13] The latter process provides opportunities for metal ion sensors with some degree of selectivity via the donor–acceptor spectral overlap. There is a considerable interest in the use of resonance energy transfer, because excitation energy can be transported over molecular distances within intervals of time which coincide with typical fluorescence lifetimes. Thus, energy transfer may be employed for the detection of the acceptors in the donor environment, and also for motion and organization studies of many systems of medical or biological importance.[14]

Resonance energy transfer was originally described by Förster[15] for the case of the dipole–dipole interaction and homogeneous media and then developed for more complicated systems by many researchers.[16–21] In the general description[21] it is assumed that the energy transfer rate $w(R)$ at the distance R between donor and acceptor is

$$w(R)=\frac{1}{\tau_D}\left(\frac{R_0}{R}\right)^s. \tag{1}$$

The parameter s in Eq. (1) equals 6 for dipole–dipole, 8 for dipole–quadrupole, and 10 for quadrupole–quadrupole interaction. τ_D is the fluorescence lifetime of the donor in the absence of any quencher. The critical transfer distance R_0 is for dipole–dipole interaction defined by the overlap integral:

$$R_0^6=\frac{9000\ln(10)K^2\Phi_0}{128\pi^5 N_A n^4}\int_0^\infty \frac{F_d(\tilde{\nu})\epsilon(\tilde{\nu})}{\tilde{\nu}^4}\,d\tilde{\nu}. \tag{2}$$

Here Φ_0 is the emission quantum yield of the donor in the absence of the acceptor, K is the orientation factor (K^2 equal to 0.67 for freely rotating donor and acceptor molecules), n is the refractive index of

the solvent. $F_d(\tilde{\nu})$ describes the emission intensity of the donor and $\epsilon(\tilde{\nu})$ is the extinction coefficient of the acceptor at the wave number $\tilde{\nu}$.

Resonance energy transfer being the additional channel of the donor depopulation influences the donor decay law $I(t)$. The rate of energy transfer $w(R)$ strongly depends on R for a particular donor–acceptor pair (1), thus the acceptor distribution around the donor molecule $\rho(R)$ significantly influences $I(t)$. For the small acceptor concentrations ($p \ll 1$, where p is the probability of having one acceptor in each site)[21,22] the relation between $\rho(R)$ and $I(t)$ is given by

$$I(t) = I_0 \exp[-t/\tau_D] \times \exp\left(-p \int dR \rho(R)\{1-\exp[-tw(R)]\}\right). \tag{3}$$

The factor $\exp[-t/\tau_D]$ describes fluorescence accompanying the energy transfer. Formula (3) is the key equation in this area and shows the potential of the energy transfer to reflect the morphology of the medium.

The analytical evaluation of the integral from Eq. (3) has only been obtained for a homogeneous distribution of acceptors in L-dimensional media. In this case

$$\rho_L(R) = L V_L \rho R^{L-1}, \tag{4}$$

where V_L is the volume of the unit sphere in L dimensions and $p\rho$ has a meaning of the number of acceptors per volume unit. Insertion of (1) and (4) into (3) gives

$$I(t) = I_0 \exp[-t/\tau_D] \times \exp[-V_L p \rho R_0^L \Gamma(1-L/s)(t/\tau_D)^{L/s}]. \tag{5}$$

This general solution contains several particular cases considered in earlier articles. We will now discuss some of these.

2.1 THREE DIMENSIONAL MEDIUM ($L=3$) AND DIPOLE–DIPOLE INTERACTION ($S=6$)

This case, previously analyzed by Förster,[15] gives the very well known formula

$$I(t) = I_0 \exp[-t/\tau_D - (4/3)\pi^{3/2} p \rho R_0^3 (t/\tau_D)^{1/2}] = I_0 \exp[-t/\tau_D - \gamma_A (t/\tau_D)^{1/2}], \tag{6}$$

where $\gamma_A = [A]/C_A$ and

$$C_A = \frac{3}{4\pi^{3/2} R_0^3 N_A} \tag{7}$$

is the three-dimensional (3D) critical molar acceptor concentration and $[A]$ is the actual molar concentration of the acceptors in the sample. N_A is the Avogadro number.

The relative donor quantum yield in Förster energy transfer can be expressed at small quencher concentrations as

$$\frac{\Phi}{\Phi_0} = 1 - \pi^{1/2}(\gamma_A/2). \tag{8}$$

The initial Förster model for 3D media was developed by various authors in the regions where it breaks down. When the rate of energy transfer from donor–donor is comparable to that from donor–acceptor, the probability of quenching by the acceptor is enhanced due to ''self'' resonance energy transfer between donors, thus allowing the excitation energy to sample the environment of several donors some of which are more efficiently quenched by virtue of their statistically denser arrangement of surrounding acceptors. According to Huber[16,17] including this process modifies Eq. (6) to the form

$$I(t) = I_0 \exp[-t/\tau_D - (\gamma_D/\sqrt{2} + \gamma_A)(t/\tau_D)^{1/2}]. \tag{9}$$

$\gamma_D = [D]/C_D$, where $[D]$ is the actual donor concentration and C_D is the critical donor concentration defined by

$$C_D = \frac{3}{4\pi^{3/2}(R_0^{DD})^3 N_A}, \tag{10}$$

where R_0^{DD} is the critical transfer distance for donor–donor energy transfer. The correction of the donor decay law due to the diffusion of the donor and acceptor molecules was calculated by Gösele.[18,19] If it is assumed that the mutual diffusion coefficient for donors and acceptors is D then

$$I(t) = I_0 \exp[-t/\tau_D - 4\pi D r_F [A] N_A t - \gamma_A (t/\tau_D)^{1/2}], \quad r_F > r_{AD} \tag{11}$$

and

$$I(t) = I_0 \exp[-t/\tau_D - 4\pi D r_{AD} [A] N_A t - 8 r_{AD}^2 [A] N_A (\pi D t)^{1/2}], \quad r_F < r_{AD}. \tag{12}$$

Here r_{AD} is the collision radius (immediate energy transfer is assumed), and r_F is an effective trapping radius

$$r_F \approx 0.676 \left(\frac{R_0^6}{\tau_D D}\right)^{1/4}. \tag{13}$$

2.2 TWO-DIMENSIONAL MEDIUM ($L=2$) AND DIPOLE–DIPOLE INTERACTION ($S=6$)

For this case formula (5) has the form

$$I(t)=I_0\exp[-t/\tau_D-\pi\Gamma(2/3)p\rho R_0^2(t/\tau_D)^{1/3}]$$
$$=I_0\exp[-t/\tau_D-\gamma'_A(t/\tau_D)^{1/3}], \quad (14)$$

where $\gamma'_A=[A]'/C'_A$ and

$$C'_A=\frac{3}{\pi\Gamma(2/3)R_0^2N_A} \quad (15)$$

is the 2D critical molar acceptor concentration and $[A]'$ is the 2D actual molar acceptor concentration. Formula (14) may be similarly developed to include donor–donor transfer and diffusional effects.

2.3 THREE-DIMENSIONAL MEDIUM ($L=3$) AND ARBITRARY S

The result for this case was found by Inokuti and Hirayama[20]

$$I(t)=I_0\exp[-t/\tau_D-(4/3)\pi p\rho R_0^3\Gamma(1-3/s)\times(t/\tau_D)^{3/s}]$$
$$=I_0\exp[-t/\tau_D-\gamma_A\pi^{-1/2}\Gamma(1-3/s)(t/\tau_D)^{3/s}]. \quad (16)$$

This donor decay law applies for the higher order interactions between donors and acceptors. It is worth noting that for $s\neq 6$ R_0 is no longer defined by the overlap integral (2).

2.4 ARBITRARY L AND DIPOLE–DIPOLE INTERACTION ($S=6$)

This case concerns the acceptors distributed on fractal geometries. Assuming the general formula for the acceptor distribution (4) we obtain

$$I(t)=I_0\exp[-t/\tau_D-V_Lp\rho R_0^L\Gamma(1-L/6)(t/\tau_D)^{L/6}]$$
$$=I_0\exp[-t/\tau_D-B(t/\tau_D)^{L/6}], \quad (17)$$

where

$$B=V_Lp\rho R_0^L\Gamma(1-L/6) \quad (18)$$

is a time-independent constant. It is essential to mention that all donor decay functions discussed here can be conveniently expressed as the product of an exponent and stretched exponent, i.e.,

$$F(t)=F_0\exp[-\alpha t-\beta t^{\sigma}]. \quad (19)$$

The analysis of the parameters α, β, and σ obtained from fitting the experimental donor fluorescence decay to the dependence (19) for the set of the samples of increasing acceptor concentration allows the most appropriate kinetic model to be found. However, all the models discussed above are only strictly applicable under well defined kinetic conditions and in the case of complex heterogeneous environments such as permeable polymer matrices like Nafion™ or in biological material such as whole cells or sub-cellular structures they can only be considered as approximate. The key question is: To what extent are they useful descriptions in biological media?

3 EXPERIMENT

DTDCI (Lambda Physik), propylene glycol (Fluka), and the transition metal salts $CuSO_4\cdot 5H_2O$ (BDH) and $NiCl_2\cdot 6H_2O$ (Aldrich) were used as obtained. Nafion™ 117 film (Aldrich) was initially boiled in concentrated nitric acid for 30 min to remove impurities, and then boiling water for 90 min. To obtain the Na^+ form, the Nafion™ film was immersed in 1 M aqueous NaOH solution for at least 10 h.

Solutions in propylene glycol were prepared as follows. The crystalline DTDCI was first added to a volumetric flask, made into solution with methanol, and placed in an ultrasonic bath for 15 min. The required amounts of DTDCI in methanol were then pipetted into the 25 ml volumetric flasks. After the methanol was removed by nitrogen gas, the transition metal salt was added and the flask was filled with the propylene glycol and briefly sonicated.

For film preparation the water solution of DTDCI was prepared in a small beaker and the water swollen Nafion™ film was put into this beaker for 5–10 min while stirring. After the film was rinsed with pure water it was put into the aqueous solution of the appropriate transition metal salt and the solution was mixed for 15 min. Because of its anionic nature the Nafion™ film will remove all the metal ions onto the film.

The absorption measurements were performed using a Perkin Elmer Lambda 2 UV/VIS spectrophotometer, and fluorescence spectra were recorded with a Shimadzu RF-540 fluorometer. All measurements were performed at room temperature. Fluorescence decay functions were measured using the technique of time correlated single photon counting.[23] A Hamamatsu PLP-01 diode laser operated at 10 MHz repetition rate was used for excitation and a Philips PM 2257B photomultiplier[24] was used for detection. The diode laser gave an instrumental pulse width of ~390 ps full width half maximum (FWHM). The excitation wavelength for all measurements was 670 nm, and emission was collected at $\lambda>715$ nm. Prism polarizers were used at the ''magic angle'' to eliminate rotational effects. The maximum number of counts in a channel was 10^4 recorded at a channel width of 20 ps. Data analysis was performed using nonlinear least-squares with the IBH iterative reconvolution library, which incorporates a chi-squared goodness of fit criterion.

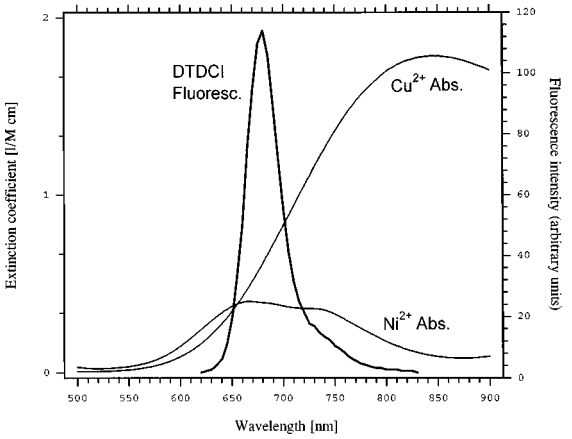

Fig. 1 Fluorescence spectra of DTDCI in propylene glycol compared with the absorption spectra of hydrated metal ions.

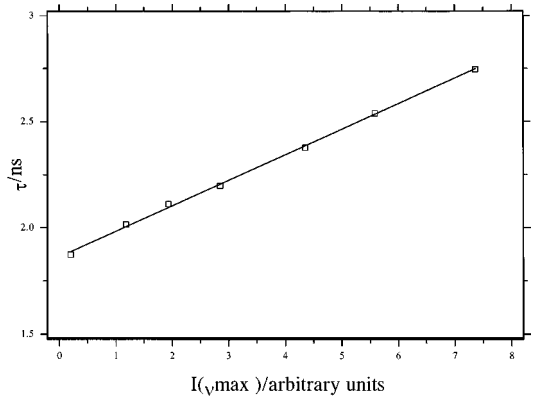

Fig. 2 The self-absorption of DTDCI in propylene glycol. τ is the measured fluorescence lifetime and $I(\tilde{\nu}_{max})$ the peak absorption coefficient.

4 RESULTS AND DISCUSSION

4.1 MEASUREMENTS OF THE PROPYLENE GLYCOL SAMPLES

Propylene glycol was chosen as the model bulk solvent for which a 3D homogeneous distribution of the acceptor molecules can be assumed. The absorption spectra of the studied transition metal ions ($Cu^{2+}\cdot 5H_2O$ and $Ni^{2+}\cdot 6H_2O$) and the fluorescence spectra of DTDCI in propylene glycol are presented in Figure 1. The absorption spectra were obtained for salt concentrations of 0.1 M in 1 cm pathlength cuvettes. The spectroscopic critical transfer distances R_0^{sp} obtained from the spectral overlap according to Eq. (2) are 19 Å for DTDCI-$Cu^{2+}\cdot 5H_2O$ and 17 Å for the DTDCI-$Ni^{2+}\cdot 6H_2O$ system. Because of the uncertainty in quantum yield measurement ($\Phi_0 \approx 0.67$) and the errors in the concentration of the samples, we estimate that the error in R_0^{sp} reaches ± 1 Å.

The time-resolved measurements of the DTDCI fluorescence decay function in propylene glycol indicated a marked lifetime dependence on the solute concentration. The decay is monoexponential and the lifetime increases with concentration, indicating the presence of radiative self-absorption. According to Birks[25] the relation between the lifetime τ and the dye concentration $[D]$ may be written in the following form:

$$1-\frac{\tau_M}{\tau}=\eta[D], \tag{20}$$

where τ_M is the fluorescence lifetime at infinite dilution (i.e., without self-absorption effects) and η is the proportionality coefficient. Converting Eq. (20) and replacing $\eta[D]$ with $\eta' I(\tilde{\nu}_{max})$ where $I(\tilde{\nu}_{max})$ is the maximum absorption coefficient and η' the appropriate proportionality coefficient gives

$$\tau=\tau_M+\eta'[\tau I(\tilde{\nu}_{max})]. \tag{21}$$

The linear dependence τ vs $\tau I(\tilde{\nu}_{max})$ predicted here and also experimentally determined for DTDCI in propylene glycol (Figure 2) provides evidence of self-absorption. Estimation of τ_M gives 1.86 ± 0.08 ns.

The quenching data obtained in this study were initially fitted to a monoexponential function and then to the simplest 3D Förster function [Eq. (6)]. The results for quenching by copper ions are presented in Table 1 and Figure 3. The unquenched sample gives a perfectly monoexponential decay with a lifetime $\tau_D = 1.85$ ns. When the quencher concentration increases the best-fit exponential decay times decrease, and the reduced chi-squared values increase up to more than 5. This excludes a monoexponential model of the kinetics in terms of only collisional quenching as the mechanism for the decrease in τ_D. Fitting to the Förster decay law gives constant values of τ_D for different copper ion concentrations and a linear increase of γ_A vs $[Cu^{2+}\cdot 5H_2O]$ indicating good agreement with the Förster model. Less than perfect values of χ^2 obtained here are attributed to experimental errors

Table 1 Kinetic parameters obtained from a monoexponential and Förster analysis of the fluorescence quenching of DTDCI in propylene glycol by $Cu^{2+}\cdot 5H_2O$ ions.

	Monoexp.		Förster (3D) [Eq. (6)]		
$[Cu^{2+}\cdot 5H_2O]$/ 0.01 M	τ/ns	χ^2	τ_D/ns	γ_A	χ^2
0.00	1.85	0.96	1.83	0.032	0.96
1.25	1.64	1.72	1.85	0.274	1.15
2.50	1.46	3.04	1.84	0.538	1.25
3.75	1.35	3.93	1.85	0.728	1.14
5.00	1.21	5.43	1.85	1.004	1.23

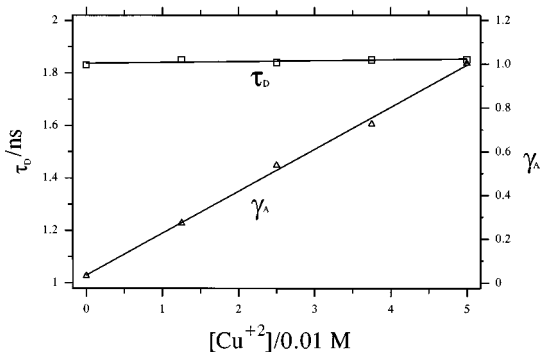

Fig. 3 Dependence of Förster parameter γ_A and fluorescence lifetime τ_D on metal ion concentration for DTDCI quenched by copper ions in propylene glycol.

rather than to the inappropriateness of the model, because the chi-squared values do not increase with the quencher concentration.

The kinetic critical transfer distance R_0^{kin} calculated from the slope of the γ_A vs $[Cu^{2+}\cdot 5H_2O]$ in terms of Eq. (7) is equal to 18±1 Å and is lower than the expected $R_0^{\text{sp}}=19\pm1$ Å. However, R_0^{sp} was calculated for an orientational factor $K^2=0.667$, which is only valid for free and fast rotating donor and acceptor molecules. K^2 for the rigid system is equal to 0.476.[26] The appropriate value of K^2 for propylene glycol solution at room temperature lies somewhere between these two values. Assuming $K^2=0.476$ we obtain $R_0^{\text{sp}}=18\pm1$ Å which is in good agreement with R_0^{kin}.

The dependence $R_0^{\text{kin}}<\cong R_0^{\text{sp}}$ shows that there is no more quenching than expected from the Förster model. Thus the Huber model [Eq. (9)] does not apply here. Also, the same value of τ_D for different quencher concentrations and for the unquenched sample indicates that diffusion does not play any role in the quenching kinetics.

To summarize this section, quenching of DTDCI by hydrated copper ions in propylene glycol exhibits well behaved Förster kinetics. This provides a good starting point for the study of the quenching kinetics of this dye in more complicated environments and by other acceptors.

Data obtained for the nickel ions as a quencher fitted to a monoexponential decay and to a 3D Förster decay are presented in Table 2 and Figure 4. The fluorescence lifetime of the unquenched sample equals 1.90 ns and is slightly longer than the lifetime estimated for infinite dilution. Therefore the results obtained for this system may be to some extent contaminated by the radiative self-absorption of DTDCI.

The decrease of τ_D with the nickel ion concentration increase means, in contradiction to the quenching by copper ions, the simple Förster model is inappropriate. The observed effect suggests the influence of diffusion and may be treated in terms of the Gösele model [Eqs. (11) and (12)]. The linear

Table 2 Kinetic parameters obtained from a monoexponential and Förster analysis of the fluorescence quenching of DTDCI in propylene glycol by $Ni^{2+}\cdot 5H_2O$ ions.

	Monoexp.		Förster (3D) [Eq. (6)]		
$[Ni^{2+}\cdot 6H_2O]$/ 0.01 M	τ/ns	χ^2	τ_D/ns	γ_A	χ^2
0.0	1.90	1.04	1.92	0.024	1.03
0.5	1.91	1.10	1.95	0.046	1.08
1.0	1.77	1.42	1.91	0.170	1.18
1.5	1.78	1.35	1.92	0.170	1.12
2.0	1.71	1.55	1.89	0.232	1.15
2.5	1.71	1.56	1.90	0.276	1.15
3.0	1.64	1.81	1.89	0.288	1.22
3.5	1.62	1.53	1.82	0.316	1.03
4.0	1.56	2.12	1.83	0.378	1.16
4.5	1.55	2.11	1.83	0.398	1.07
5.0	1.49	2.63	1.83	0.480	1.21

dependence of $\tau_D^{-1}([A])$ required in the Gösele model was found for this case to have a correlation coefficient $r=0.91$ (see Figure 8). The critical point is the relation between the trapping radius r_F and collisional distance r_{AD} for DTDCI and $Ni^{2+}\cdot 6H_2O$ molecules. The direct calculation of these two parameters is not possible and therefore Eqs. (11) and (12) will be analyzed separately.

Let us assume first that the diffusion coefficient is low enough that Eq. (11) applies. Inserting (13) into (11) gives the formula

$$D^{3/4}=0.1177\,\frac{(\tau_D^{-1}([A])-\tau_D^{-1}(0))\,\tau_D{}^{1/4}}{(R_0^{\text{sp}})^{3/2}[A]N_A}, \quad (22)$$

where $\tau_D([A])$ is the time parameter obtained from fitting to Eq. (6) for the quencher concentration $[A]$

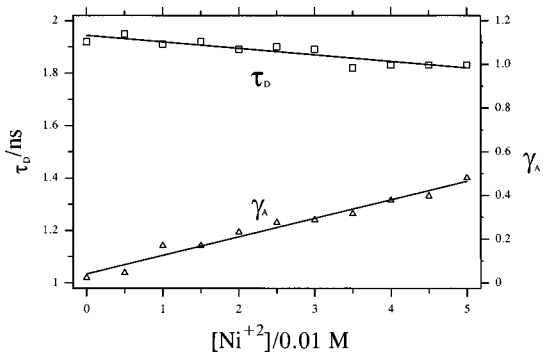

Fig. 4 Dependence of Förster parameter γ_A and fluorescence lifetime τ_D on metal ion concentration for DTDCI quenched by nickel ions in propylene glycol.

and $\tau_D(0)=\tau_D$. The diffusion coefficient D estimated from the dependence $\tau_D^{-1}([A])$ and Eq. (22) equals 1.93×10^{-7} cm^2/s and seems to be reasonable for a solvent like propylene glycol. The trapping radius calculated from Eq. (13) for this diffusion coefficient is $r_F=35$ Å. However, the meaning of the γ_A parameter in Eq. (11) is the same as in the Förster model (6) and R_0^{kin} obtained from the slope of the γ_A vs $[Ni^{2+}\cdot 6H_2O]$ dependence is 13 ± 1 Å. (The correction of γ_A resulting from $\tau_D([A]) \neq \tau_D(0)$ has been taken into account in this calculation.) This value is markedly lower from the expected $R_0^{\text{sp}}=17$ Å. Assuming again rotational rigidity of the system decreases R_0^{sp} to 16 Å which is still inconsistent with the kinetic value. Therefore in our opinion Eq. (11) is not fully appropriate in this case and may be only considered as an approximation to the actual kinetics.

Now we can turn to Eq. (12). By comparison of this equation with the experimental dependencies $\tau_D^{-1}([A])$ and γ_A the diffusion coefficient D and collisional radius r_{AD} may be calculated from

$$D^{3/2}=\frac{(\tau_D^{-1}([A])-\tau_D^{-1}(0))^2\tau_D^{1/2}(0)}{2\pi^{3/2}[A]N_A\gamma_A} \tag{23}$$

and

$$r_{AD}=\frac{(\tau_D^{-1}([A])-\tau_D^{-1}(0))}{4\pi D[A]N_A}. \tag{24}$$

The diffusion coefficient D obtained from (23) equals 3.1×10^{-7} cm^2/s and collisional radius from Eq. (24) is $r_{AD}=22$ Å.

The values of D obtained from Eqs. (11) and (12) do not differ dramatically, indicating that the real value probably lies between them. Assuming $D \approx 2.5\times10^{-7}$ cm^2/s, we obtain $r_{AD}\approx27$ Å and $r_F \approx 33$ Å. This result means that none of the Gösele functions properly describe the quenching of DTDCI by hydrated nickel ions in propylene glycol, because none of the parameters r_{AD} and r_F is markedly larger than the other. However Eq. (11) seems to be more appropriate, because the observed decrease in τ_D may be explained in part as the result of the diffusion and also as the consequence of the decreasing role of reabsorption as the concentration of acceptors increases. Therefore the diffusion slightly modifies the dominance of the Förster energy transfer kinetics. Nevertheless, this analysis shows that for the application of resonance energy transfer as the mechanism of a selective (spectral overlap) and sensitive (large gradient γ_A vs $[A]$) sensor a self-absorption process should be avoided and condition $r_F \gg r_{AD}$ must be observed. This may be achieved by: applying a low donor concentration, minimizing the diffusion coefficient D, using small molecules (small r_{AD}), and using donor–acceptor pairs of large spectral overlap (large R_0).

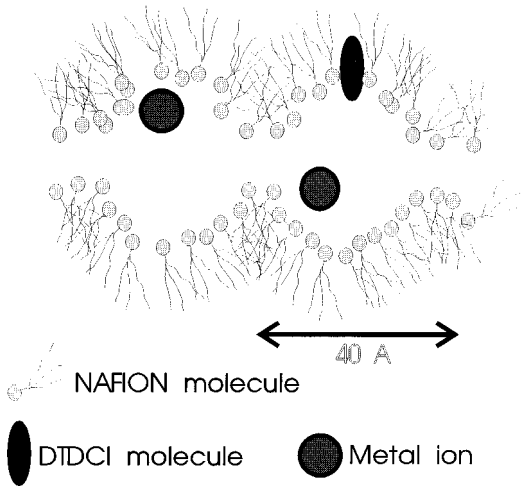

Fig. 5 The Nafion™ porous structure with the location of the metal ions and DTDCI molecules.

Otherwise quenching will be dominated by the collisional processes. These observations constitute useful ground rules when implementing Förster energy transfer in a biomedical context.

4.2 MEASUREMENTS OF THE NAFION™ SAMPLES

Nafion™ 117 perfluorinated ionomer membrane has the following chemical formula:

$$[-(CF_2-CF_2)_m-CF-CF_2-]_n$$
$$|$$
$$(O-CF_2-CF-CF_3)_k$$
$$|$$
$$O$$
$$|$$
$$CF_2-CF_2-SO_3H$$

$m=5$ to 13.5
$n\simeq1000$
$k=1,2,3\ldots$

The fluorocarbon backbone of the membrane provides exceptional chemical, thermal, and mechanical stability, while the sulfonate head groups provide a porous structure with ion exchange, water storage, and swelling capabilities. Nafion™ has been investigated both as a remote sensing medium and for its own structural determination using fluorescent probes.[3,27–31] Previously we have shown that probes fluorescing in the UV/VIS could be used for selectively detecting metal ions on the basis of nonradiative energy transfer.[11,28] In the present work we use the NIR dye DTDCI incorporated in Nafion™ (Figure 5) as a model microhet-

erogeneous environment for energy transfer sensing in a medium which simulates a scattering medium such as tissue.

We have found that the fluorescence intensity of DTDCI in water swollen Nafion™ decreases with time elapsed from when the sample is prepared to almost nothing in approximately 20–30 h. The shape of the fluorescence decay also changes in time and the mean fluorescence lifetime increased from 1.95 ns for a freshly prepared sample to about 3.10 ns after approximately 80 min. In this initial period of time the shape of the decay changes during data collection, so good fits to any theoretical curve cannot be expected. We attribute this initial instability to the diffusion of the dye molecules within the Nafion™ sample and to changes in the dye microenvironment during this process. After the molecules are settled in the polymer, the decay function becomes stable and can be well described by a monoexponential when unquenched and by Förster kinetics when quenched with metal ions. This is a very useful starting point for an organic dye in such a complex medium. All measurements were performed for samples prepared at least 2 h previously. The samples were then stable during the first 6–8 h after the measurements began, but the intensity of fluorescence decreased to an unmeasurable value within approximately 20–30 h irrespective of the presence of any quencher.

The instability of DTDCI described above is not only a characteristic of the samples in Nafion™ swollen by water. Similar effects were observed for DTDCI incorporated to HEMA:AA:PEGDMA (2 hydroxyethylmethylacrylate:acrylic acid:poly(400) ethylene glycol dimethyl acrylate) polymer swollen by water.

In quenching studies of DTDCI in Nafion™ the polymer was doped from solution at approximately twice the concentration of the solute, as compared with the propylene glycol measurements. The reason for this was the necessity to provide enough fluorescence intensity for time-resolved measurements at the higher quencher concentrations. The τ_D values for unquenched Nafion™ samples were greater than in propylene glycol (Tables 3 and 4: results for zero quencher concentration). This reflects the change of environment, not least of which is the increased self-absorption due to the dye being more closely confined within the polymer pores. Note also that the thin Nafion™ films used (~0.2 mm) precludes distortion of the fluorescence decays due to photon migration at multiple scattering sites on the nanosecond timescales of interest.

The quenching data obtained for both copper and nickel ions in Nafion™ are similar and therefore will be discussed here together. The kinetic parameters obtained from fitting to monoexponential and 3D Förster [Eq. (6)] functions are presented in Table 3 and Figure 6 for copper and in Table 4 and Figure 7 for nickel ions. The reduction in the best-fit exponential decay times with increase in quencher concentration observed here indicate diffusional quenching. However, increasing chi-squared values indicate more than a collisional mechanism is present. Much better chi-squared values were obtained for the 3D Förster model, although the decreasing $\tau_D([A])$ dependence implies more complicated kinetics than described in Eq. (6).

The dependencies of $\tau_D^{-1}([A])$ for both ions (Figure 8) were found to be linear with correlation coefficients r equal to 0.96 for copper and 0.83 for nickel ions, which is consistent with the Gösele

Table 3 Kinetic parameters obtained from a monoexponential and Förster analysis of the fluorescence quenching of DTDCI in Nafion™ 117 by $Cu^{2+}\cdot 5H_2O$ ions.

	Monoexp.		Förster (3D) [Eq. (6)]		
$[Cu^{2+}\cdot 5H_2O]$/ 0.01 M	τ/ns	χ^2	τ_D/ns	γ_A	χ^2
0.00	3.03	1.18	3.12	0.068	1.11
0.59	2.93	1.08	3.00	0.054	1.04
1.18	2.83	1.15	2.95	0.092	1.05
1.78	2.77	1.38	2.93	0.120	1.19
2.37	2.47	2.00	2.82	0.304	1.10
2.96	2.46	2.22	2.87	0.344	1.11
3.55	2.35	2.44	2.79	0.384	1.13
4.14	2.27	3.33	2.80	0.486	1.51
4.73	2.11	3.55	2.69	0.572	1.26

Table 4 Kinetic parameters obtained from a monoexponential and Förster analysis of the fluorescence quenching of DTDCI in Nafion™ 117 by $Ni^{2+}\cdot 5H_2O$ ions.

	Monoexp.		Förster (3D) [Eq. (6)]		
$[Ni^{2+}\cdot 6H_2O]$/ 0.01 M	τ/ns	χ^2	τ_D/ns	γ_A	χ^2
0.00	3.10	1.05	3.10	0.000	1.04
1.48	2.74	1.14	2.93	0.150	0.93
2.95	2.54	1.89	2.90	0.310	1.13
3.69	2.47	1.95	2.83	0.344	1.07
4.43	2.37	2.37	2.86	0.440	1.03
5.17	2.29	2.56	2.78	0.464	1.17
5.90	2.14	3.90	2.88	0.712	1.09
6.64	2.01	2.78	2.87	0.858	1.19
7.38	1.95	4.57	2.79	0.462	1.12
8.12	1.90	4.82	2.78	0.922	1.09

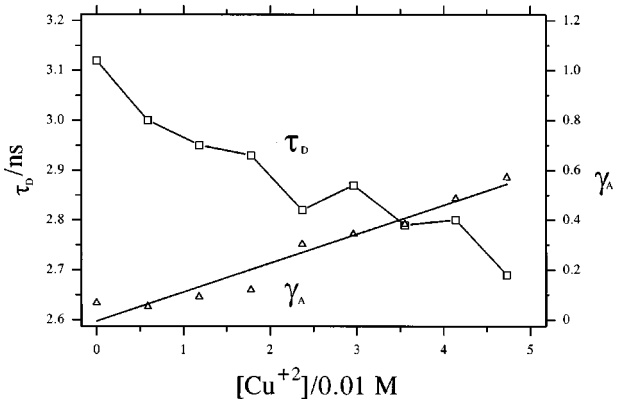

Fig. 6 Dependence of Förster parameter γ_A and fluorescence lifetime τ_D on metal ion concentration for DTDCI quenched by copper ions in Nafion™.

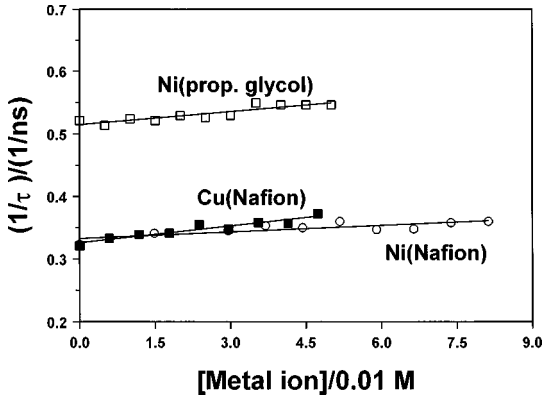

Fig. 8 The τ_D^{-1}([Metal ion]) dependence for τ_D parameters obtained from fitting of the fluorescence decays to Eq. (6).

model. To clarify the role of diffusion in Nafion™, calculations similar to those for nickel in propylene glycol were performed. The parameters obtained on the basis of the kinetic data and Eqs. (11) and (12) are presented in Table 5. Relation $r_F > r_{AD}$ obtained for both quenchers suggest the validity of Eq. (11) however the r_F parameters are again not markedly greater than r_{AD} as the influence of the diffusion might be expected to reveal. Moreover, R_0^{kin} are lower than R_0^{sp} even when rigidity of the system is assumed. Interestingly enough, the system for which larger D was detected (copper ions) also exhibits a larger discrepancy between spectroscopic and kinetic values of the critical transfer distances. Therefore, similar to the propylene glycol samples, we attribute the experimentally observed reduction in critical transfer distance (when the data is fitted to 3D Förster decay) to the influence of the mutual donor–acceptor diffusion. The collisional distances r_{AD} estimated here for the pairs DTDCI–$Cu^{2+}\cdot 5H_2O$ and DTDCI–$Ni^{2+}\cdot 6H_2O$ seem to be reasonable, bearing in mind the relatively large dimensions of a NIR dye such as DTDCI.

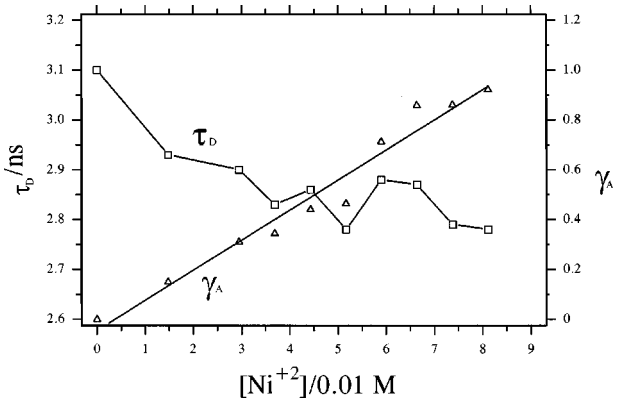

Fig. 7 Dependence of Förster parameter γ_A and fluorescence lifetime τ_D on metal ion concentration for DTDCI quenched by nickel ions in Nafion™.

In the analysis performed so far it was assumed that the factor L/s in Eq. (5) [or power σ in Eq. (19)] is equal to 1/2. A physical meaning of this assumption is a random 3D distribution of the acceptors around donors and the dipole–dipole character of the donor–acceptor interaction. In homogeneous environments such as propylene glycol these assumptions are reasonable, but not in the porous structure of the Nafion™ film. First, because acceptors are located only in the water pools of the film the acceptor distribution function may not be random. Second, because the donor–acceptor distances within the film may be closer than in the bulk solution and their interaction more complicated than the assumed dipole–dipole interaction. Any of these factors can lead to the deviation of L/s from 1/2.

In order to investigate whether such a deviation appears in Nafion™, fitting to the general formula (5) has been performed. The fluorescence decays for both propylene glycol and Nafion™ samples were analyzed for fixed τ_D parameters. Results are presented in Table 6 (propylene glycol) and Table 7

Table 5 The parameters obtained on the basis of the kinetic data and Eqs. (11) and (12).

Quenching ion:	$Cu^{2+}\cdot 5H_2O$	$Ni^{2+}\cdot 6H_2O$
$R_0^{\text{sp.}}$ (free-rot.)/$R_0^{\text{sp.}}$ (rigid)	19 Å/18 Å	16 Å/15 Å
Equation (11):		
D	4.8×10^{-7} cm^2/s	2.2×10^{-7} cm^2/s
r_F	29.0 Å	27.9 Å
$R_0^{\text{kinet.}}$	14 Å	14 Å
Equation (12):		
D	8.4×10^{-7} cm^2/s	3.0×10^{-7} cm^2/s
r_{AD}	16.7 Å	20.0 Å

Table 6 The parameters L/s obtained from fitting of the fluorescence decays of DTDCI in propylene glycol to Eq. (5).

Acceptor conc./0.01 M	L/s	χ^2
Cu^{2+}	τ_D=1.85 ns (Fixed)	
0	1	1.16
1.25	0.532	1.23
2.5	0.481	1.47
3.75	0.508	1.42
5	0.489	1.50
Ni^{2+}	τ_D=1.90 ns (Fixed)	
0	1	1.16
1.0	0.524	1.17
2.0	0.484	1.17
3.0	0.547	1.21
4.0	0.578	1.20
4.5	0.580	1.08
5.0	0.514	1.42

Table 7 The parameters L/s obtained from fitting of the fluorescence decays of DTDCI in Nafion™ to Eq. (5).

Acceptor conc./0.01 M	L/s	χ^2
Cu^{2+}	τ_D=3.03 ns (Fixed)	
0	1	1.16
0.59	0.667	1.05
1.18	0.714	1.05
1.77	0.641	1.22
2.37	0.651	1.12
2.96	0.609	1.14
3.55	0.644	1.16
4.14	0.619	1.59
4.73	0.589	1.40
Ni^{2+}	τ_D=3.10 ns (Fixed)	
0	1	1.09
1.48	0.707	0.92
3.69	0.665	1.08
4.43	0.629	1.03
5.17	0.651	1.17
5.90	0.577	1.09
6.64	0.562	1.21
7.38	0.588	1.16
8.12	0.584	1.11

(Nafion™). The dependence of the L/s factor as a function of the ion concentration is plotted in Figure 9. L/s for propylene glycol samples remains around 1/2 confirming 3D dipole–dipole energy transfer, while in the Nafion™ L/s parameter, it is well above 1/2 for lower ion concentrations and then gradually approaches 1/2 for higher concentrations. This cannot be caused by any deviation of the kinetics from the Förster model, because in this case the effect should be stronger for the higher ion concentration. In our opinion the changes in L/s are observed because the ions have no access to the part of the donors in the Nafion™ sample and these donors exhibit monoexponential decay (L/s for monoexponential function is 1). Therefore the real decay function describes hybrid kinetics of the form

$$I(t)=I_1([A])\exp\left(-\frac{t}{\tau_D}\right)+I_2([A]) \times\exp\left[-\frac{t}{\tau_D}-2\gamma\left(\frac{t}{\tau_D}\right)^{1/2}\right], \qquad (25)$$

with the ratio $I_1([A])/I_2([A])$ decreasing with the acceptor concentration $[A]$ increase. This observation goes some way in explaining the discrepancies found between measured and actual metal ion concentrations on Nafion™ based metal ion sensors.[11,12]

To summarize, some slight deviations from the Förster model detected in the Nafion™ samples can be explained by the influence of diffusion, and also the hybrid kinetics resulting from the hindered access of the ions to some of the donor molecules. This raises the interesting question as to whether or not it is possible to determine the distribution func-

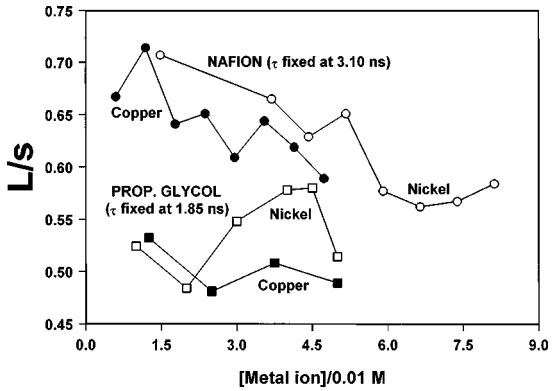

Fig. 9 The L/s parameters obtained from fitting of the fluorescence decays to the general formula (5).

tion for acceptors from the L/s ratio. If so then this may have further application in the monitoring of biomedical analytes.

5 CONCLUSIONS

The measurements reported above confirm the potential use of NIR dyes as infrared fluorescence sensors. Carbocyanine dyes such as DTDCI may be used successfully to detect metal ions in microheterogeneous media such as tissue. However, the samples studied were found to be unstable for longer periods of time. The photochemical instability and complex photophysics of carbocyanine dyes are undoubtedly limiting their application in medical sensing and highlights the fact that, as in other areas, the development of better NIR dyes is of paramount importance if the potential advantage of working with fluorescence in the NIR is to be realized. Nevertheless, our results show that by understanding the quenching kinetics many potential sources of systematic errors, such as dye aggregation and diffusion, can be overcome.

Acknowledgment

The authors wish to thank the EPSRC for research support.

REFERENCES

1. J. R. Lakowicz and B. Maliwal, ''Optical sensing of glucose using phase-modulation fluorimetry,'' *Anal. Chim. Acta* **271**, 155–164 (1993).
2. S. A. Sopper and Q. L. Mattingly, ''Steady state and picosecond laser fluorescence studies of nonradiative pathways in tricarbocyanine dyes: Implications to the design of near-IR fluorochromes with high fluorescence efficiencies,'' *J. Am. Chem. Soc.* **116**, 3744–3752 (1994).
3. J.-M. Zen, M. Lipowska, and G. Patonay, ''Near infrared probe for in situ characterization of nafion thin films,'' *J. Appl. Polym. Sci.* **46**, 1167–1176 (1992).
4. J. C. Mialocq, J. Jaraudias, and P. Goujon, ''Picosecond spectroscopy of pinacyanol (1,1′-diethyl-2,2′-monocarbocyanine chloride),'' *Chem. Phys. Lett.* **47**, 123–126 (1977).
5. D. Andrews-Wilberforce and G. Patonay, ''Fluorescence quenching studies of near-infrared fluorophores,'' *Appl. Spectrosc.* **43**, 1450–1455 (1989).
6. G. Hungerford, D. J. S. Birch, and R. E. Imhof, ''Spark source infrared fluorometry,'' *Proc. SPIE* **1640**, 262–270 (1992).
7. D. J. S. Birch and G. Hungerford, ''Instrumentation for red/near-infrared fluorescence,'' in *Topics in Fluorescence Spectroscopy*, J. R. Lakowicz, Ed. Vol. 4, Plenum, New York (1994).
8. J.-M. Zen and G. Patonay, ''Near-infrared fluorescence probe for pH determination,'' *Anal. Chem.* **63**, 2934–2938 (1991).
9. S. J. Lehotay, P. A. Johnson, T. E. Barber, and J. D. Winefordner, ''Ultralow detection limit of a near-infrared dye by diode-lased-induced fluorescence on a flowing stream,'' *Appl. Spectrosc.* **44**, 1577–1579 (1990).
10. E. Laitinen, P. Russkanen-Jarvinen, U. Rempel, V. Helenius, and J. E. I. Korppi-Tommola, ''Rotation correlation time as a measure of microviscosity of excited state isomerization reactions of three cyanine dyes in n-alcohol solutions,'' *Chem. Phys. Lett.* **218**, 73–80 (1994).
11. D. J. S. Birch, A. S. Holmes, and M. Darbyshire, ''Intelligent sensor for metal ions based on fluorescence resonance energy transfer,'' *Meas. Sci. Technol.* **6**, 243–247 (1995).
12. D. J. S. Birch, O. J. Rolinski, and D. Hatrick, ''Fluorescence lifetime sensor of copper ions in water,'' *Rev. Sci. Instrum.* **67**, 2732–2737 (1996).
13. J. R. Lakowicz, *Principles of Fluorescence Spectroscopy*, Plenum, New York (1983).
14. Ch. D. Stubbs and B. W. Williams, ''Fluorescence in membranes,'' in *Topics in Fluorescence Spectroscopy*, J. R. Lakowicz, Ed. Vol. 3, Plenum, New York (1992).
15. T. Förster, ''Experimentelle und theoretische Untersuchung des zwischenmolekularen Ubergangs von Elektronenanregungsenergie,'' *Z. Naturforsch.* **4a**, 321–327 (1949).
16. D. L. Huber, ''Fluorescence in the presence of traps,'' *Phys. Rev. B* **20**, 2307–2314 (1979).
17. D. L. Huber, ''Donor fluorescence at high trap concentration,'' *Phys. Rev. B* **20**, 5333–5338 (1979).
18. U. Gösele, M. Hauser, U. K. A. Klein, and R. Frey, ''Diffusion at long range energy transfer,'' *Chem. Phys. Lett.* **34**, 519–522 (1975).
19. U. K. A. Klein, R. Frey, M. Hauser, and U. Gösele, ''Theoretical and experimental investigations of combined diffusion and long-range energy transfer,'' *Chem. Phys. Lett.* **41**, 139–142 (1976).
20. M. Inokuti and F. Hirayama, ''Influence of energy transfer by the exchange mechanism on donor luminescence,'' *J. Chem. Phys.* **43**, 1978–1989 (1965).
21. A. Blumen, ''Excitation transfer from a donor to acceptors in condensed media: a unified approach,'' *Nuovo Cimento* **63B**, 50–58 (1981).
22. J. Klafter, J. M. Drake, and A. Blumen, ''Excited state dynamics in low-dimensional systems,'' in *Kinetics and Catalysis in Microheterogeneous Systems*, M. Grätzel and K. Kalyanasundaram, Eds., Chap. 14, Marcel Dekker, Inc., New York (1991).
23. D. J. S. Birch and R. E. Imhof, ''Time-domain fluorescence spectroscopy using time correlated single-photon counting,'' in *Topics in Fluorescence Spectroscopy*, J. R. Lakowicz, Ed., Vol. 1, Plenum, New York (1991).
24. D. J. S. Birch, G. Hungerford, B. Nadolski, R. E. Imhof, and A. D. Dutch, ''Time correlated single-photon counting fluorescence decay studies at 930 nm using spark source excitation,'' *J. Phys. E: Sci. Instrum.* **21**, 857–862 (1988).
25. J. B. Birks, *Photophysics of Aromatic Molecules*, Wiley-Interscience, New York (1970).
26. R. E. Dale and J. Eisinger, ''Intramolecular energy transfer and molecular conformation,'' *Proc. Natl. Acad. Sci. USA* **73**, 271–273 (1976).
27. P. C. Lee and D. Meisel, ''Photophysical studies of pyrene incorporated in Nafion membranes,'' *Photochem. Photobiol.* **41**, 21–26 (1985).
28. A. S. Holmes, M. Lopez, O. J. Rolinski, D. J. S. Birch, and M. Darbyshire, ''A fluorescence energy transfer for metal ions,'' *Proc. SPIE* **2388**, 171–181 (1995).
29. F. V. Bright, G. E. Poirier, and G. M. Hieftje, ''A new ion sensor based on fiber optics,'' *Talanta* **35**, 113–118 (1988).
30. I. Nataga, R. L. E. Banks, and Y. Okamoto, ''Energy transfer from donor to acceptor ions in perfluorosulfonate membranes,'' *Macromolecules* **16**, 903–905 (1983).
31. P. C. Lee and D. Meisel, ''Luminescence quenching in the cluster network of perfluorosulfonate membrane,'' *J. Am. Chem. Soc.* **102**, 5477–5481 (1980).